Experimental determination of the B-T phase diagram of $YBa_2Cu_3O_{7-\delta}$ to 150 T for $B \perp c$

J. L. O'Brien*
National Pulsed Magnet Laboratory and Semiconductor Nanofabrication Facility, School of Physics, University of New South Wales, Sydney 2052, Australia

H. Nakagawa
Institute for Solid State Physics, University of Tokyo, 7-22-1 Roppongi, 106 Tokyo, Japan

A. S. Dzurak, R. G. Clark, B. E. Kane, N. E. Lumpkin, and R. P. Starrett
National Pulsed Magnet Laboratory and Semiconductor Nanofabrication Facility, School of Physics, University of New South Wales, Sydney 2052, Australia

N. Muira
Institute for Solid State Physics, University of Tokyo, 7-22-1 Roppongi, 106 Tokyo, Japan

E. E. Mitchell
CSIRO, Division of Telecommunications and Industrial Physics, Lindfield 2070, Australia

J. D. Goettee and D. G. Rickel
Los Alamos National Laboratory, Los Alamos, New Mexico 87545

J. S. Brooks
Department of Physics, Florida State University, Tallahassee, Florida 32310
(Received 27 September 1999)

The B-T phase diagram for thin film $YBa_2Cu_3O_{7-\delta}$ with B parallel to the superconducting layers has been constructed from GHz transport measurements to 150 T. Up to 110 T the upper critical field is found to be linear in T and in remarkable agreement with extrapolation of the longstanding result of Welp *et al.* arising from magnetization measurements to 6 T. Beyond this a departure from linear behavior occurs at $T=74$ K, consistent with previous low-temperature data. Evidence for a transition from a high-T regime dominated by orbital effects, to a low-T regime, where paramagnetic limiting drives the quenching of superconductivity, is seen.

Recent magnetotransport measurements on high-T_c cuprates have provided invaluable information in building a complete picture of these materials, essential to the development of a rigorous theory for the phenomenon of high-temperature superconductivity. For example, divergence in the upper critical field at low T has been reported in overdoped $Tl_2Ba_2CuO_6$,[1] $Bi_2Sr_2CuO_y$,[2,3] and $La_{2-x}Sr_xCuO_4$.[3] Such results have provided the impetus for considerations of unconventional behavior in the anisotropic high-T_c cuprates such as reentrant superconductivity and the possibility to exceed the paramagnetic limit.[4] These measurements have typically relied on millisecond pulsed fields to observe upper critical fields, which exceed the range ($\sim$35 T) of steady field magnets. For higher-T_c materials such as optimally oxygen-doped $YBa_2Cu_3O_{7-\delta}$ (YBCO) ($T_c \sim 90$ K) access to the normal state requires magnetic fields well in excess of those generated by ms pulsed systems except for T very near T_c. Explosive flux compression technology has been used to access this high-field regime,[5–8] providing evidence for paramagnetic limiting of the upper critical field in YBCO for B parallel to the superconducting layers ($\mathbf{B} \perp \mathbf{c}$).[5,7] However, such measurements are extremely difficult and opportunities to make them are few. Single-turn coil magnetic field generators have also been used to make transport measurements on thin-film YBCO.[9] While these systems do not produce fields in the range of flux compression techniques, they do allow for systematic, repeatable measurements to be made as the destruction of the coil does not damage the sample or cryostat. Nevertheless, transport measurements remain difficult since the peak field is reached in a few μs and the maximum dB/dt exceeds 10^8 T/s.

Previous flux compression measurements on thin film YBCO with $\mathbf{B} \perp \mathbf{c}$ (Ref. 5) gave an onset of dissipation $B_{ons} = 150$ T and an upper critical field $B_{c2} = 240$ T at 1.6 K. This B_{c2} is significantly smaller than $B_{c2}^{\perp}(0) = 674$ T predicted by Welp *et al.*[10] who applied the Werthamer-Helfand-Hohenberg[11] (WHH) formalism, accounting for orbital effects only, following measurements of the slope dB_{c2}/dT near T_c. This large discrepancy has been interpreted[5] in terms of the Clogston-Chandresekhar paramagnetic limit B_p,[12,13] which arises when the Zeeman energy exceeds the superconducting energy gap Δ_0, thus destroying the Cooper pair singlet state. Within BCS theory $B_p = \gamma T_c$, with $\gamma = 1.84$ T/K,[12] which, for optimally doped YBCO gives $B_p \sim 170$ T. In stark contrast to these results for in-plane magnetic fields, measurements[6,9] in the alterna-

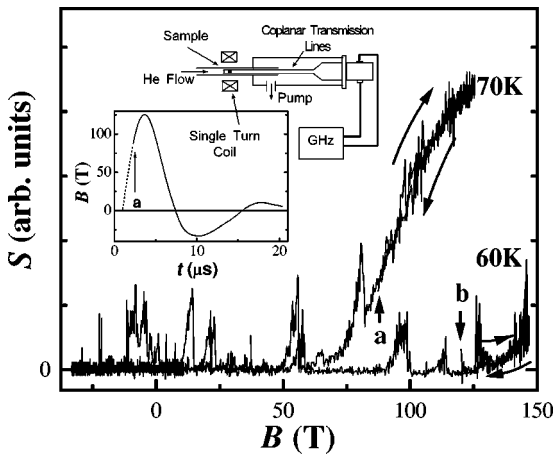

FIG. 1. Raw GHz transmission S, with $\mathbf{B}\perp\mathbf{c}$, shown for times after the point marked a (b) for $T=70$ K (60 K). Before these times, data are obscured by electrical noise arising from the discharge of the capacitor bank. Arrows indicate the direction of the field sweep. The insets show the experimental configuration for measurements and the field profile of the single-turn coil.

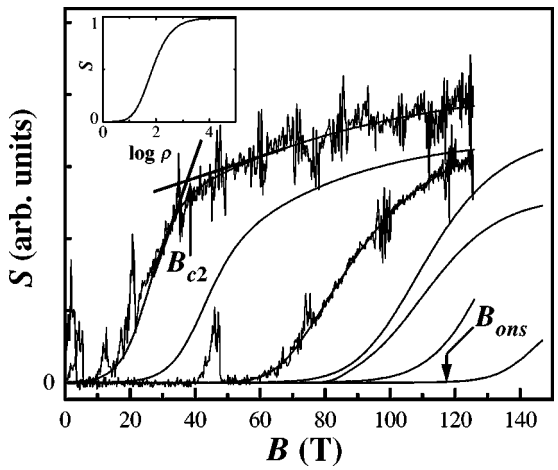

FIG. 2. Fits to raw magnetoresponse $S(B)$ data for $T=80$ K, 78 K, 74 K, 72 K, 66 K, 65 K, and 60 K with onset fields increasing, respectively. Traces have been scaled vertically for clarity (Ref. 17). Raw data are shown for comparison for $T=80$ K and 74 K. Definitions of B_{ons} and B_{c2} are indicated. The S response to sample sheet resistivity ρ (in Ω) is shown in the inset.

tive and more widely studied configuration, $\mathbf{B}\|\mathbf{c}$, have mapped out the entire phase diagram in good agreement with the WHH model.

Here we report transport measurements that have allowed the *B-T* phase diagram of YBCO to be constructed for $B<150$ T in the $\mathbf{B}\perp\mathbf{c}$ orientation, greatly extending previous magnetization measurements to 6 T.[10] Although explosive flux compression techniques have previously been used to access this regime,[5,7] the single-turn coil system allows systematic measurements to be made on a single sample with both rising and falling magnetic field. Measurements on thin-film samples were made using a GHz technique[14] in a single-turn coil system[15] generating fields to 150 T. The superconducting-normal transition was observed to be an equilibrium process, evidenced by the absence of any measurable hysteresis between up and down B sweeps. Above $T=74$ K B_{c2} is found to be linear in T with the slope $\alpha=dB_{c2}/dT$ corresponding closely to that found in magnetization measurements.[10] Below 74 K a departure from this slope is observed and is understood as arising from a transition from three-dimensional (3D) behavior where orbital effects quench superconductivity to 2D behavior where paramagnetic limiting dominates.

The experimental configuration is shown in the inset to Fig. 1. A symmetric triplet coplanar transmission line (CTL) carries a microwave signal, $\nu=0.8$–1 GHz, past the sample and the transmission S is modulated by the resistivity ρ of the sample. Full details of the experimental arrangement are set out in Ref. 14. A flow of cold He gas gives access to T in the range 7–300 K with sample T monitored by a AuFe-Chromel thermocouple mounted on the back side of the substrate. Two thermocouples mounted side by side on the same sample gave consistent readings to within 0.5 K. Discharge of a 40 kV capacitor bank into a 10-mm-diameter single-turn copper coil generated fields to 150 T and the copper coil was vaporized in the process, leaving the sample and cryostat intact.[15]

A YBCO film, thickness 250 nm, $T_c=87.2$ K and critical current $J_c=3.14$ MA/cm^2 at 77 K, was grown by on-axis dc magnetron sputtering on a MgO (001) substrate, with the c-axis oriented in the growth direction, at $T=770\,^{\circ}$C in an argon-oxygen atmosphere with a deposition time ~ 90 min. The film was etched to produce a 20 μm strip perpendicular to the CTL to match the sample resistance to the characteristic impedance of the CTL $Z=50\Omega$. A 50 nm dielectric layer of Si_3N_4 separated the film and CTL so that coupling to the sample was capacitive. This eliminates the need for Ohmic contacts to the sample, which can be problematic in pulsed fields.[16]

Raw transmission S as a function of B is plotted for $T=60$ K and 70 K in Fig. 1. The single-turn coil system produces a number of cycles of B prior to destruction (Fig. 1 inset). The absence of any hysteresis in the data was consistently observed in several samples over a range of temperatures, providing confidence in the critical-field information obtained and in its comparison with equilibrium models for high-T_c behavior.

In the superconducting state the sample acts as an equipotential across the CTL, completely attenuating the microwave signal, resulting in zero transmission. As the applied field B drives the sample normal, S increases with increasing ρ. A model of this response is shown in the inset to Fig. 2, calculated assuming capacitive coupling across the 50 nm Si_3N_4 dielectric layer to a 2D sheet of electrons.[14] Sharp noise spikes in the data are attributed to GHz emission from the plasma produced in vaporization of the single-turn coil and are predominantly in the direction of increasing S since the technique measures transmitted power (as opposed to voltage).

Fits to the raw data for the decreasing B sweep, which take into account the positive-going nature of the noise spikes, are shown in Fig. 2. The fits are purely for display purposes and the functional form has no physical significance. We define B_{c2} as the intersection of the tangent to the transmission curve in the transition region and that immediately after it, following Ref. 1 on the basis that this gives values close to the 90% criterion and in good agreement with

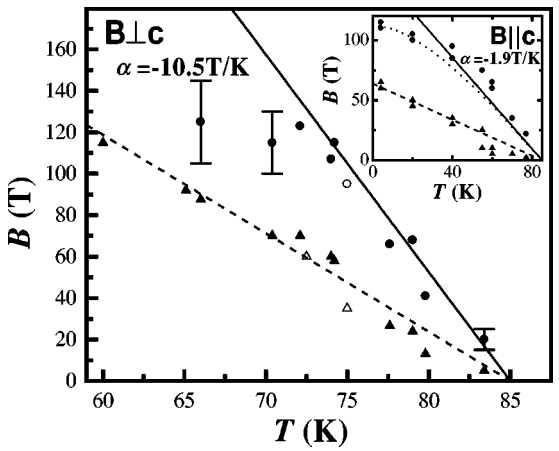

FIG. 3. *B-T* phase diagram for YBCO with $\mathbf{B}\perp\mathbf{c}$. Solid circles and triangles represent B_{c2} and B_{ons}, respectively. Open symbols arise from measurements on a second sample fabricated from the same film. The inset shows the equivalent phase diagram taken from Nakagawa *et al.* (Ref. 9) with $\mathbf{B}\|\mathbf{c}$. In both cases the solid line shows the slope $\alpha = dB_{c2}/dT$ determined from magnetization measurements (Ref. 10) and the dashed line is simply a guide to the eye.

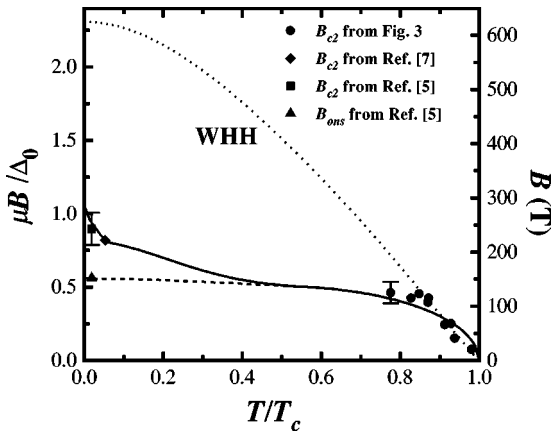

FIG. 4. Full phase diagram for YBCO for $\mathbf{B}\perp\mathbf{c}$. The B_{c2} data from Fig. 3 is replotted along with low *T* data from Refs. 5 and 7. The dotted line is the WHH phase boundary (Ref. 11) calculated considering orbital effects only. The solid line is the second-order phase boundary, and the dashed line, the first-order BCS-FFLO phase boundary taken from Ref. 27, which considers only coupling between the spins and the applied *B*. The reduced field is calculated with the energy gap defined as $\Delta_0 = 2.14T_c$ (Ref. 27).

tunneling data. For the lowest *T* measurements, determining B_{c2} becomes more difficult because there is less saturation region. We find, however, that the form of the transition is essentially the same for all *T*. We estimate the error in B_{c2} by constructing extrema tangents to the transmission curve after the transition, while the tangent in the transition region is well defined. B_{ons} is defined as the point at which the transmission departs from $S=0$.

Figure 3 shows the *B-T* phase diagram for $T>60$ K, with B_{ons} and B_{c2} values determined from the complete data set, a subset of which is shown in Fig. 2. In magnetization measurements up to 6 T on single crystal YBCO with $\mathbf{B}\perp\mathbf{c}$, B_{c2} was found to be linear in *T* with $dB_{c2}/dT = -10.5$ T/K.[10] The extrapolation of this slope α is plotted in Fig. 3 and we find that our data follow it closely down to $T=74$ K where $B_{c2}\sim 100$ T. Note that as in Ref. 10 this line intersects the *T* axis slightly below T_c as do the B_{ons} data. This is allowed for in Fig. 4 below.

Discrepancies between B_{c2} determined from resistive measurements and either magnetization[10] or specific heat[18] data have been reported, and it has been argued that the latter two better probe the mean-field B_{c2} than do resistivity measurements.[3] With the definition of B_{c2} used here for GHz measurements in the high-field regime the remarkable agreement we find with dB_{c2}/dT determined from low-field magnetization measurements suggests that, in our case, probing resistivity yields a B_{c2} in accordance with the mean-field value.

Although WHH theory includes paramagnetic and spin-orbit effects, in this paper we consider the model arising from orbital effects only, as applied by Welp *et al.*[10] Whereas this model predicts a departure from the slope α only at low *T*, we see clear evidence for a departure below 74 K. Previous measurements by Nakagawa *et al.*[9] provide convincing evidence for the applicability of this model to YBCO for $\mathbf{B}\|\mathbf{c}$ (Fig. 3 inset). Near T_c their data agree well with the dB_{c2}/dT slope determined previously[10] and application of the WHH result:

$$B_{c2}(0) = 0.7T_c(dB_{c2}/dT)|_{T_c} \tag{1}$$

gives $B_{c2}^{\|}(0) = 112$ T, in close agreement with that measured. Indeed, this agreement extends over the entire phase boundary (dotted line in Fig. 3 inset). A larger dB_{c2}/dT for the case $\mathbf{B}\perp\mathbf{c}$, due to anisotropy in coherence lengths ξ_c out of plane and ξ_{ab} in plane, leads to a significantly larger $B_{c2}^{\perp}(0) > 600$ T in this model. A deviation well below this value is clear in Fig. 3, however. The good agreement between WHH and experiment for $\mathbf{B}\|\mathbf{c}$ and the departure from expected behavior for $\mathbf{B}\perp\mathbf{c}$ suggests that a different mechanism may be responsible for the quenching of superconductivity in the latter case. Misalignment of *B* has been considered but cannot explain the low *T* results of Ref. 5 or the deviation observed here.

Paramagnetic-limited upper critical fields have been observed in UPd_2Al_3,[19] while $B_{c2} > B_p$ has recently been seen in $(TMTSF)_2PF_6$,[20] where TMTSF denotes tetramethyltetraselenafulvalene. The results in Refs. 5 and 7 provided evidence for paramagnetic limiting in a high-T_c material. The paramagnetic limit in YBCO is expected to occur at $B_p \sim 170$ T, well above $B_{c2}^{\|}(0) = 110$ T measured for $\mathbf{B}\|\mathbf{c}$,[9] and well below $B_{c2}^{\perp}(0) = 640$ T predicted for $\mathbf{B}\perp\mathbf{c}$ with $T_c = 87$ K (see Ref. 10). The difference between WHH and experiment for $\mathbf{B}\perp\mathbf{c}$ is shown clearly in Fig. 4 where the WHH phase boundary and the data from Fig. 3 are plotted on a full phase diagram. The departure from this phase boundary is consistent with the results from flux compression measurements[5,7] (also plotted[21]) and provides further evidence for paramagnetic limiting of B_{c2} for $\mathbf{B}\perp\mathbf{c}$.

A possible fit to the data of Refs. 5 and 7 for $\mathbf{B}\perp\mathbf{c}$ has been obtained[22] by including spin-orbit and paramagnetic parameters in the WHH and Maki[23] models. While it is instructive to apply these 3D models, their applicability to in-plane critical fields in layered superconductors is brought into question by analysis,[24] which has found that there is a nonzero temperature $T^* < T_c$ below which the normal cores of

the vortices are smaller than the lattice constant d, defined by $\xi_c(T^*)=d/\sqrt{2}=8.5$ Å. Below T^* orbital effects should no longer provide a mechanism for quenching of superconductivity and, in the absence of paramagnetic and spin-orbit effects, B_{c2} would be infinite.

A 3D-2D crossover is expected to occur near T^* when ξ_c becomes smaller than the interplane spacing. $\xi_c(70\ \mathrm{K}) \sim 8$ Å is the separation between pairs of CuO planes,[25] and $\xi_c(80\ \mathrm{K}) \sim d=12$ Å is the lattice constant.[26] The departure from the linear behavior of $B_{c2}(T)$ observed here at $T=74$ K is almost midway between these two characteristic temperatures. A theory which includes the finite thickness of the superconducting layers in the cuprates, but neglects paramagnetic effects,[26] predicts a crossover in $B_{c2}(T)$ from linear to nonlinear behavior at $T=0.9T_c \sim 78$ K. As described above, orbital effects should become negligible after a 3D-2D crossover. $B_{c2}(T)$ is then expected to increase *more* rapidly with decreasing T, in contrast to the behavior observed here. It may, however, be significant that the departure from linear behavior at 74 K is near the expected position of this dimensional crossover.

The phase diagram predicted[27] for a layered d-wave superconductor with $\mathbf{B}\perp\mathbf{c}$, which accounts for coupling between the spins and the applied B is compared with experiment in Fig. 4. The only free parameter is the g factor, which is set equal to 2. The agreement between this theory[27] and the low-T data[5,7] is surprisingly good, supporting the conjecture that quenching of superconductivity is driven by paramagnetic effects at low T. In contrast, the data close to T_c is better fitted by WHH, which is to be expected since the theory in Ref. 27 does not consider orbital effects. For intermediate temperatures, below 74 K, the data tend to lie above the phase boundary predicted in Ref. 27. This is also suggested by B_{ons} at 60 K, which implies a $B_{c2}(T)$ above this phase boundary. While it is possible to fit the data of Fig. 4 using theories, that include orbital, spin-orbit, and paramagnetic effects,[28] we consider just the two extremes of orbital-only and paramagnetic-only theories to illustrate the transition from one regime to the other. The phase diagram predicted in Ref. 27 and shown in Fig. 4 includes a finite momentum or Fulde-Ferrel-Larkin-Ovchinnikov[29] (FFLO) superconducting state and we note that B_{ons} for the data of Ref. 5 coincides with the position of the first-order phase transition between the zero momentum and FFLO state. This may not be accidental since the superfluid density and J_c may be lower in the FFLO phase.[30]

In conclusion, we have found that for $\mathbf{B}\perp\mathbf{c}$ the upper critical field in YBCO follows the WHH phase boundary for $T>74$ K. For lower T the data are consistent with a theory,[27] which accounts for coupling of the spins to the applied B. This suggests a transition from a high-T regime where superconductivity is governed by orbital effects to a low-T regime where paramagnetic effects dominate. We note that the departure from linear behavior occurs close to the expected position of a 3D-2D crossover. Combined with the data of Refs. 5 and 7 this constitutes strong evidence for the experimental realization of paramagnetic limiting in a high-T_c cuprate superconductor.

We thank K. Yang, S.L. Sondhi, and R.H. McKenzie for detailed discussions and comments on this manuscript, B. Sankrithyan, who grew the film, and researchers at the Megagauss Laboratory, ISSP, Tokyo University for expert technical help and advice. This work was supported by the Australian Research Council and Grant-in-Aid for International Scientific Research of the Ministry of Education, Science and Culture, Japan.

*Electronic address: job@phys.unsw.edu.au

[1] A. P. Mackenzie *et al.*, Phys. Rev. Lett. **71**, 1238 (1993).
[2] M. S. Osofsky *et al.*, Phys. Rev. Lett. **71**, 2315 (1993).
[3] Y. Ando *et al.*, Phys. Rev. B **60**, 12 475 (1999).
[4] A. G. Lebed and K. Yamaji, Phys. Rev. Lett. **80**, 2697 (1998).
[5] A. S. Dzurak *et al.*, Phys. Rev. B **57**, 14 084 (1998).
[6] J. L. Smith *et al.*, J. Low Temp. Phys. **95**, 75 (1994).
[7] J. D. Goettee *et al.*, Physica B **194-196**, 1805 (1994).
[8] A. I. Bykov *et al.*, Physica B **211**, 248 (1995); A. I. Golovashkin *et al.*, *ibid.* **177**, 105 (1992).
[9] H. Nakagawa *et al.*, Physica B **246-247**, 429 (1998).
[10] U. Welp *et al.*, Phys. Rev. Lett. **62**, 1908 (1989).
[11] N. R. Werthamer, E. Helfand, and P. C. Hohenberg, Phys. Rev. **147**, 295 (1966).
[12] A. M. Clogston, Phys. Rev. Lett. **9**, 266 (1962).
[13] B. S. Chandrasekhar, Appl. Phys. Lett. **1**, 7 (1962).
[14] B. E. Kane *et al.*, Rev. Sci. Instrum. **68**, 3843 (1997).
[15] N. Miura, Physica B **201**, 40 (1994).
[16] For further sample fabrication details see, N. E. Lumpkin *et al.*, Physica B **246-247**, 40 (1998).
[17] Because the CTL impedance is T dependent, the GHz frequency is tuned slightly differently for each trace such that the attenuation of the signal is complete (i.e., $S=0$) for $B=0$. As a result the saturation levels are slightly different for each trace.
[18] A. Carrington, A. P. Mackenzie, and A. Tyler, Phys. Rev. B **54**, 3788 (1996).
[19] K. Gloos *et al.*, Phys. Rev. Lett. **70**, 501 (1993).
[20] I. J. Lee *et al.*, Phys. Rev. Lett. **78**, 3555 (1997).
[21] B_{c2} was obtained in Ref. 7 by taking the precise zero crossing of the imaginary component of the saturated GHz signal, guided by theoretical arguments. However the most significant feature in the data defining the transition occurs at significantly lower B and B_{c2} obtained from this feature, as in Fig. 2, is plotted here.
[22] J. S. Brooks *et al.*, in *Proceedings of the Eighth International Conference on Megagauss Magnetic Field Generation and Related Topics, Tallahassee, 1998*, edited by H. Schneider-Muntau (World Scientific, Singapore, in press).
[23] K. Maki, Physics (Long Island City, N.Y.) **1**, 127 (1964).
[24] R. A. Klemm, A. Luther, and M. R. Beasley, Phys. Rev. B **12**, 877 (1975).
[25] G. Burns, *High Temperature Superconductivity* (Academic Press, Boston, 1992), p. 154.
[26] T. Schneider and A. Schmidt, Phys. Rev. B **47**, 5915 (1993).
[27] K. Yang and S. L. Sondhi, Phys. Rev. B **57**, 8566 (1998).
[28] R. A. Klemm (private communication).
[29] P. Fulde and R. A. Ferrell, Phys. Rev. **135**, A550 (1964); A. I. Larkin and Yu. N. Ovchinnikov, Zh. Éksp. Teor. Fiz. **47**, 1136 (1964) [Sov. Phys. JETP **20**, 762 (1965)].
[30] K. Yang and S. L. Sondhi (private communication).